Int. J. Heat Mass Transfer. Vol. 30, No. 5, pp. 869–880, 1987
Printed in Great Britain

0017–9310/87 $3.00 + 0.00

Periodic B-spline basis for quasi-steady periodic inverse heat conduction

G. P. FLACH and M. N. ÖZIŞIK
Mechanical and Aerospace Engineering Department, North Carolina State University, Raleigh, NC 27695-7910, U.S.A.

(*Received* 2 *June* 1986 *and in final form* 3 *September* 1986)

Abstract—A method based on the use of periodic B-splines and the integral transform technique is proposed for the solution of quasi-steady periodic linear inverse heat conduction problems. Previous approaches based on a finite Fourier series representation of the unknown surface condition are best suited to smooth time variations of the surface condition. Now, using a B-spline representation, problems with discontinuities or abrupt variations in the surface condition can be handled readily. The versatility of the B-spline basis allows prior information concerning the general functional behavior of the surface condition to be better incorporated into the model.

1. INTRODUCTION

THE DETERMINATION of a periodically varying surface temperature or heat flux from discrete measurements of the quasi-steady interior temperature has numerous practical applications, including, among others, the analysis of internal combustion engines [1, 2], prediction of thermal contact conductance of periodically contacting surfaces [3, 4] and periodic on–off heating processes [5, 6]. Many of the quasi-steady periodic inverse heat conduction problems (IHCP) arising from such applications are linear and involve simple geometries. For instance, experimental apparatus for the measurement of thermal contact conductance between quasi-steady periodically contacting surfaces typically involve two one-dimensional rods which contact at one end and are held at a known condition at the opposite ends [3, 4]. Measurements are taken at an interior location(s) in each rod to avoid disturbing the surface properties under consideration. The analysis requires the determination of the unknown temperature and heat flux at each of the contacting surfaces, i.e. the solution of quasi-steady periodic inverse heat conduction problems. Unless the thermal properties vary significantly over the temperature range of interest the IHCP is linear. Wendland investigated the heat transfer characteristics of a closed system subjected to periodic conditions. Part of the analysis involved the solution of a one-dimensional quasi-steady periodic linear IHCP [7]. Some investigations of internal combustion engines have also involved the solution of a one-dimensional periodic linear IHCP [1, 2].

The current analytical approaches for the solution of such quasi-steady periodic linear IHCP make use of a finite Fourier series for the representation of the unknown surface condition [1, 2, 7–9]. We are not aware of any numerical methods developed for periodic IHCP. The analytical methods utilizing a finite Fourier series basis are restricted to problems involving a smooth variation in time of the surface condition. However, there are applications such as periodically contacting surfaces and periodic on–off heating processes which involve a discontinuous time variation of surface temperature, hence the use of a trigonometric basis for the estimated surface temperature cannot accurately accommodate the actual physical situation. Furthermore, it is important to have as few parameters as possible in the model representing the unknown surface condition in order to minimize the effects of measurement errors, that is, an efficient representation is desirable. In this regard, a Fourier series representation is frequently very inefficient. If the surface condition variation is abrupt at any point in the time domain, a large number of sine–cosine frequencies is required to adequately model the situation. The resulting estimates are much more sensitive to measurement errors than necessary due to the inefficient Fourier series representation.

In the present work, a versatile periodic B-spline basis (periodic piecewise continuous polynomial basis) for the unknown surface condition coupled with an efficient integral transform technique and splitting-up procedure is proposed. The approach is applicable to quasi-steady periodic linear IHCP corresponding to the direct problems solvable by the integral transform approach advanced in ref. [10]. More specifically, multidimensional problems in rectangular, cylindrical or spherical geometry with heat generation and boundary conditions of the first, second and/or third kind can be treated. Arbitrary order (constant, linear, cubic, etc.) for the polynomial pieces and continuity requirements between each piece is available from a single, unified formulation. The desired B-spline representation is obtained by simply choosing a set

NOMENCLATURE

a_j, b_j	Fourier series coefficients
$\mathbf{B}^*$	vector of periodic B-spline basis functions
$\mathbf{c}^*$	vector of periodic B-spline coefficients
$d_j^*(x,t)$	basis functions for the interior temperature
$\mathbf{D}^*$	matrix of interior temperature basis functions at the measurement times, t_i
$\det(\hat{f})$	deterministic error in $\hat{f}$
$E(\cdot)$	expected or average value operator
$f(t)$	periodic surface temperature
$\mathbf{G}$	matrix associated with autoregressive errors
$k-1$	order of the B-spline functions
l	number of intervals in the B-spline basis
n	number of normalized B-spline functions
n^*	number of periodic B-spline functions, $n - v_1 = N_d$
N	number of measured interior temperatures T_i
N_d	number of data points needed to define the periodic B-spline coefficients; dimension of the periodic B-spline basis
$q(t)$	periodic surface heat flux
r	arbitrary constant in integral (A1)
$\mathbf{s}$	knot sequence defining $B_{i,k}(t)$ in integral (A1)
SSE	sum of the squared estimated errors
$\text{sto}(\hat{f})$	stochastic error in $\hat{f}$
t	time
$T(x,t)$	interior temperature
u_i	independent random variable component of autoregressive error model
v	arbitrary constant in integral (A1)
$\text{var}(\hat{f})$	variance in $\hat{f}$
x	spatial coordinate
x_1	position of the interior temperature measurements
z_{1j}, z_{2j}	defined by equations (A3).

Greek symbols

β_m	eigenvalues
δ	small number
ε_i	measurement errors
$\theta(x,t)$	quasi-steady periodic solution of equations (4)
v_i	number of continuity requirements at $t = \xi_i$
ξ_i	interval interface positions
ρ	constant in autoregressive error model
σ	standard deviation
τ	period of $f(t)$
$\psi(x)$	steady-state solution of equations (3).

Superscripts

T	transpose of matrix
*	associated with periodic B-spline functions
$\hat{}$	estimated quantity
$\tilde{}$	measured quantity.

Subscripts

$\hat{f}$	associated with the estimated surface temperature $\hat{f}$
$\hat{q}$	associated with the estimated surface heat flux $\hat{q}$
sto	associated with the stochastic error
u	associated with the random variable u_i.

of input constants to the common formulation. The periodic B-spline basis can accommodate discontinuities in the surface condition and derivative(s) as required by a particular application, thus making the approach very general. Also, when quantitative or qualitative information is available concerning the general functional form of the true surface condition, the B-spline basis can incorporate such information into the model to reduce the number of parameters used. The more efficient B-spline representation is then less sensitive to measurement errors, resulting in an improved estimate of the unknown surface condition. Approximate confidence bounds for the estimated surface condition are readily developed with the present formulation.

Before proceeding with the present approach, we want to point out that analytical methods for linear transient IHCP, ref. [11] for example, and numerical schemes developed for non-linear transient IHCP, such as refs. [12, 13], could also be applied to the problems we are considering, although we are not aware of any investigators doing so. However, the computations would start from some arbitrary initial condition and proceed until the quasi-steady periodic temperature distribution is established. Such an approach requires more computer time than necessary.

The versatility and accuracy of the present B-spline/integral transform approach is illustrated in a one-dimensional planar geometry for the case of an unknown temperature at one surface. Other geometries and boundary conditions can be treated just as easily. Approximate confidence bounds are developed for the estimated surface condition for both uncorrelated and correlated errors. Numerical comparisons are made with the Fourier series approach.

2. PREPARATION FOR THE INVERSE ANALYSIS

Basic to the inverse analysis is the development of a rapidly converging solution for the equivalent direct problem. To prepare such a basis, we consider a finite slab subjected to zero temperature at the surface $x = 0$ and a known periodically varying surface temperature, $f(t)$, at $x = 1$. The mathematical formulation of the quasi-steady periodic direct problem is given by

$$\frac{\partial^2 T(x,t)}{\partial x^2} = \frac{\partial T(x,t)}{\partial t} \qquad 0 < x < 1 \tag{1a}$$

$$T(0,t) = 0 \tag{1b}$$

$$T(1,t) = f(t) \tag{1c}$$

$$T(x,0) = T(x,\tau) \tag{1d}$$

where τ is the period of $f(t)$. For simplicity, we use a homogeneous boundary condition of the first kind at $x = 0$ and choose to formulate the problem in terms of a surface temperature, $f(t)$, at $x = 1$. As previously stated, the cases of boundary conditions of the second or third kind at $x = 0$ and a heat flux or ambient temperature described by $f(t)$ at $x = 1$ pose no difficulty.

To obtain a fast-converging solution to this problem, $T(x,t)$ is split-up in the following manner [14]

$$T(x,t) = \psi(x)f(t) + \theta(x,t) \tag{2}$$

where $\psi(x)$ is the solution to the following steady-state problem

$$\frac{\mathrm{d}^2\psi(x)}{\mathrm{d}x^2} = 0 \qquad 0 < x < 1 \tag{3a}$$

$$\psi(0) = 0 \tag{3b}$$

$$\psi(1) = 1 \tag{3c}$$

and $\theta(x,t)$ is the solution to the following quasi-steady periodic problem with energy generation

$$\frac{\partial^2\theta(x,t)}{\partial x^2} - \psi(x)\frac{\mathrm{d}f(t)}{\mathrm{d}t} = \frac{\partial\theta(x,t)}{\partial t} \qquad 0 < x < 1 \tag{4a}$$

$$\theta(0,t) = 0 \tag{4b}$$

$$\theta(1,t) = 0 \tag{4c}$$

$$\theta(x,0) = \theta(x,\tau). \tag{4d}$$

The solution to the steady-state problem (3) is easily obtained by direct integration. Equations (4) are solved using the integral transform technique in the manner described by Mikhailov [10]. The complete fast-converging direct solution to equations (1) is obtained as

$$T(x,t) = xf(t) + \sum_{m=1}^{\infty} \frac{-2\beta_m\cos\beta_m}{[1-\exp(-\beta_m^2\tau)]}\sin\beta_m x \times \left\{\frac{-[1-\exp(-\beta_m^2\tau)]f(t)}{\beta_m^2} + \int_0^t \exp[-\beta_m^2(t-t')]f(t')\,\mathrm{d}t' + \int_t^\tau \exp[-\beta_m^2(\tau+t-t')]f(t')\,\mathrm{d}t'\right\} \tag{5a}$$

where the eigenvalues, β_m, are given by

$$\beta_m = m\pi; \qquad m = 1,2,\ldots \tag{5b}$$

Knowing the temperature distribution, the surface heat flux at $x = 1$, $q(t)$, is computed from its definition

$$q(t) = \frac{-\partial T(1,t)}{\partial x}. \tag{6}$$

Having the solution to the direct problem established, we consider the representation of the arbitrary periodic surface temperature $f(t)$.

There are several ways to represent an arbitrary periodic function $f(t)$ over a given interval depending upon the properties of the function dictated by the application of interest. Traditional approaches utilizing a finite Fourier series representation for an arbitrary periodic function are best suited to very smooth periodic variations. Since the sine and cosine basis functions are extremely smooth (i.e. infinitely differentiable over the whole domain) and nonzero over the entire time domain (except at a finite number of points), numerous terms are required to represent a periodic variation which is not particularly smooth or even discontinuous. Even with a large number of terms in the Fourier series, oscillations still appear near discontinuities in the function or derivatives. Therefore, difficulties are experienced when approximating an arbitrary periodic function with a finite Fourier series.

Recently, the spline function approach has received considerable attention since the above difficulties can be alleviated by using less smooth (finitely differentiable) basis functions which are nonzero only locally. With the spline function approach, excellent approximations to both smooth and abrupt variations are obtained with a minimal number of basis functions. Therefore, we prefer to use the periodic polynomial spline function technique to represent $f(t)$ as a periodic piecewise continuous polynomial function of time. Accordingly, the following definitions are introduced.

$(k-1)$ ≡ the order of each polynomial piece (7a)

l ≡ the number of intervals (polynomial pieces) in each period of duration τ (7b)

ξ_i ≡ the positions of the interval interfaces or breakpoints; $i = 1$ to $l + 1$ (7c)

v_i ≡ the number of continuity conditions (i.e. continuity of function, first derivative, etc., required at each interface position, ξ_i; $i = 1$ to $l + 1$. (7d)

Once k, l, ξ_i and v_i are selected, the problem becomes one of selecting the proper basis functions, $B_j(t)$, such that the unknown surface temperature $f(t)$ is represented in the form

$$f(t) = \sum_{j=1}^{n} c_j B_j(t). \tag{8}$$

Here, the proper basis functions, $B_j(t)$, are called *normalized B-splines*. An excellent treatment of B-spline functions can be found in the monograph by de Boor [15]. For a given sequence of k, ξ_i and v_i with $v_i \leq k$ for all i, the number of B-splines, n, needed for the representation of the function is determined by the formula [15, theorem IX.1]

$$n = k + \sum_{i=2}^{l} (k - v_i) \tag{9a}$$

$$= kl - \sum_{i=2}^{l} v_i \tag{9b}$$

$$= \sum_{i=1}^{l} (k - v_i) + v_1. \tag{9c}$$

The $(k - 1)$ order B-spline functions themselves are defined by a stable, efficient recursion relationship involving the next lower order B-splines [15, p. 131], which allows us to compute the $B_j(t)$ functions. The number of data points, N_d, needed to uniquely define the coefficients c_j in the representation given by equation (8) is v_1 less than the number, n, of B-splines, because the periodicity condition for the coefficients provides an additional v_1 relations. With this consideration we write

$$N_d = n - v_1 \tag{10}$$

and the additional v_1 relationships among the coefficients c_j can be expressed as

$$c_{n - v_1 + j} = c_j; \qquad j = 1, 2, \ldots, v_1. \tag{11}$$

Thus, N_d data points together with the relationship given by equations (11) provide n relations for the determination of n unknown coefficients.

For convenience in the subsequent analysis, we prefer to contain the periodicity condition, equation (11), implicitly in the B-splines and accordingly, introduce *periodic B-splines* with the following definitions

$$B_j^*(t) \equiv \begin{cases} B_j(t) + B_{n - v_1 + j}(t); & j = 1, 2, \ldots, v_1 \\ B_j(t); & j = (v_1 + 1), (v_1 + 2), \ldots, (n - v_1) \end{cases} \tag{12a}$$

$$c_j^* \equiv c_j; \quad j = 1, 2, \ldots, (n - v_1) \tag{12b}$$

$$n^* \equiv n - v_1 = N_d \tag{12c}$$

so that equations (8) and (11) are equivalent to

$$f(t) = \sum_{j=1}^{n^*} c_j^* B_j^*(t). \tag{13}$$

Now the number of data points, N_d, required to define the coefficients c_j^* is the same as the number of coefficients, n^*.

3. ESTIMATION OF THE SURFACE TEMPERATURE

Having established the formalism for the development of a fast-converging direction solution and the representation of the unknown surface temperature, $f(t)$, using the periodic B-spline basis, we now focus our attention to the formulation of the inverse analysis concerned with estimating the unknown surface temperature from discrete measurements taken at an interior location after the quasi-steady state temperature distribution has been established. The formulation is developed in the slab geometry.

Consider a slab of thickness unity, subjected to zero temperature on the boundary $x = 0$ and to an unknown periodically varying temperature, $f(t)$, at the surface $x = 1$. Let the unknown exact surface temperature, $f(t)$, be represented formally with a periodic B-spline series in the form of equation (13)

$$f(t) = \sum_{j=1}^{n^*} c_j^* B_j^*(t) \tag{14a}$$

where the proper values have been chosen for parameters k, l, ξ_i and v_i defined by equations (7). Equation (14a) is written more compactly in matrix notation

$$f = \mathbf{B}^{*\mathrm{T}} \mathbf{c}^*. \tag{14b}$$

Substitution of representation (14a) into the direct solution (5) yields the corresponding exact interior temperature distribution in the form

$$T(x, t) = \sum_{j=1}^{n^*} c_j^* d_j^*(x, t) \tag{15a}$$

where $d_j^*(x, t)$ is defined by

$$d_j^*(x, t) \equiv x B_j^*(t) + \sum_{m=1}^{\infty} \frac{-2\beta_m \cos \beta_m}{[1 - \exp(\beta_m^2 \tau)]} \sin \beta_m x \times \left\{ \frac{-[1 - \exp(-\beta_m^2 \tau)] B_j^*(t)}{\beta_m^2} + \int_0^t \exp[-\beta_m^2 (t - t')] B_j^*(t')\, dt' + \int_0^\tau \exp[-\beta_m^2 (\tau + t - t')] B_j^*(t')\, dt' \right\}. \tag{15b}$$

The integrations appearing in equation (15b) involve an exponential multiplied with a polynomial function, $B_j^*(t')$, so the integrals can be evaluated exactly. In the Appendix we develop an efficient recursion

relationship for this purpose which is analogous to the recursion relationship used to evaluate the B-spline functions themselves. The unknown exact heat flux at $x = 1$ is obtained from equations (6) and (15a) as

$$q(t) = \sum_{j=1}^{n^*} c_j^* \left[\frac{-\partial d_j^*(1,t)}{\partial x} \right]. \tag{16}$$

Suppose N temperature measurements are taken at a single interior location x_1 at times t_i. The exact interior temperatures, $T(x_1, t_i)$, at the measurement position, x_1, and at times, t_i, are given by

$$T(x_1, t_i) \equiv T_i = \sum_{j=1}^{n^*} c_j^* d_j^*(x_1, t_i); \qquad i = 1, 2, \ldots, N \tag{17a}$$

which is expressed in the matrix form as

$$\mathbf{T} = \mathbf{D}^{*\mathrm{T}} \mathbf{c}^* \tag{17b}$$

where

$$(\mathbf{D}^*)_{ji} \equiv d_j^*(x_1, t_i). \tag{17c}$$

Suppose the actual measured data, $\tilde{T}_i$, contains errors, ε_i, such that

$$\tilde{T}_i = T_i + \varepsilon_i; \qquad i = 1, 2, \ldots, N. \tag{18}$$

For the moment, no assumptions are made concerning the measurement errors.

Now consider the estimation of $f(t)$ from the measured data, $\tilde{T}_i$. Generally, the true functional form of $f(t)$ is unknown; that is, n^* and $B_j^*(t)$ (which are defined by k, l, ξ_i, and v_i) are unknown in addition to the parameters c_j^*. To perform the inverse analysis, a functional form must be assumed for the estimated surface temperature, $\hat{f}(t)$, say, in the form

$$\hat{f}(t) = \sum_{j=1}^{\hat{n}^*} \hat{c}_j^* \hat{B}_j^*(t) \tag{19a}$$

where suitable values are chosen for the parameters $\hat{k}$, $\hat{l}$, $\hat{\xi}_i$ and $\hat{v}_i$. The matrix form of equation (19a) is preferred later in the analysis

$$\hat{f} = \hat{\mathbf{B}}^{*\mathrm{T}} \hat{\mathbf{c}}^*. \tag{19b}$$

The corresponding estimated interior temperature, $\hat{T}(x, t)$, is obtained by substituting equation (19a) into the direct solution (5) to yield

$$\hat{T}(x, t) = \sum_{j=1}^{\hat{n}^*} \hat{c}_j^* \hat{d}_j^*(x, t) \tag{20a}$$

where $\hat{d}_j^*(x, t)$ is obtained by replacing B_j^* with $\hat{B}_j^*$ in equation (15b). Analogous to equation (17b) we have

$$\hat{\mathbf{T}} = \hat{\mathbf{D}}^{*\mathrm{T}} \hat{\mathbf{c}}^* \tag{20b}$$

and the estimated heat flux is obtained from equation (20a) as

$$\hat{q}(t) = \sum_{j=1}^{\hat{n}^*} \hat{c}_j^* \left[\frac{-\partial \hat{d}_j^*(1,t)}{\partial x} \right]. \tag{21}$$

The estimated interior temperatures, $\hat{T}_i$, at the times, t_i, of the measurements are related to the measurements, $\tilde{T}_i$, by

$$\tilde{T}_i = \hat{T}_i + \hat{\varepsilon}_i; \qquad i = 1, 2, \ldots, N \tag{22a}$$

or expressed in matrix form

$$\tilde{\mathbf{T}} = \hat{\mathbf{T}} + \hat{\boldsymbol{\varepsilon}} \tag{22b}$$

$$= \hat{\mathbf{D}}^{*\mathrm{T}} \hat{\mathbf{c}}^* + \hat{\boldsymbol{\varepsilon}} \tag{22c}$$

where the quantities $\hat{\varepsilon}_i$ are the estimated errors defined by

$$\hat{\varepsilon}_i \equiv (T_i - \hat{T}_i) + \varepsilon_i; \qquad i = 1, 2, \ldots, N. \tag{23}$$

The coefficients $\hat{c}_j^*$ appearing in equations (19) can be determined by the method of least squares as now described. The sum of the squared estimated errors, SSE, is

$$\mathrm{SSE} = \hat{\boldsymbol{\varepsilon}}^{\mathrm{T}} \hat{\boldsymbol{\varepsilon}} = (\tilde{\mathbf{T}} - \hat{\mathbf{D}}^{*\mathrm{T}} \hat{\mathbf{c}}^*)^{\mathrm{T}} (\tilde{\mathbf{T}} - \hat{\mathbf{D}}^{*\mathrm{T}} \hat{\mathbf{c}}^*). \tag{24}$$

Minimization of the SSE with respect to the coefficients $\hat{c}_j^*$ yields the following system of equations for the determination of $\hat{c}^*$.

$$(\hat{\mathbf{D}}^* \hat{\mathbf{D}}^{*\mathrm{T}}) \hat{\mathbf{c}}^* = (\hat{\mathbf{D}}^* \tilde{\mathbf{T}}). \tag{25}$$

The formal solution to system (25) is

$$\hat{\mathbf{c}}^* = (\hat{\mathbf{D}}^* \hat{\mathbf{D}}^{*\mathrm{T}})^{-1} (\hat{\mathbf{D}}^* \tilde{\mathbf{T}}) \tag{26}$$

and the estimated temperature, $\hat{f}(t)$, is obtained from equations (19b) and (26) as

$$\hat{f} = \hat{\mathbf{B}}^{*\mathrm{T}} (\hat{\mathbf{D}}^* \hat{\mathbf{D}}^{*\mathrm{T}})^{-1} (\hat{\mathbf{D}}^* \tilde{\mathbf{T}}). \tag{27}$$

The quality of the estimated temperature obtained from this expression depends on the order of the piecewise polynomial, $(\hat{k} - 1)$, the number, $\hat{l}$, and positions, $\hat{\xi}_i$, of intervals and the number of continuity conditions chosen, $\hat{v}_i$. Ideally, there should be just enough flexibility in the chosen functional form for $\hat{f}(t)$ so that the overall variation indicated by the data can be accommodated without allowing $\hat{f}$ to follow the measurement errors in the data. The most common approach for selecting the basis for $\hat{f}$ in the IHCP literature, in the absence of prior knowledge about the true functional form of $f(t)$, has been to match the r.m.s. estimated error, $\sqrt{(\mathrm{SSE}/N)}$, with known statistical properties of the errors in the data [16].

First consider the standard case of uncorrelated errors with zero means and known constant variance, σ^2. The estimated or sample variance, $\hat{\sigma}^2$, is a random variable defined by

$$\hat{\sigma}^2 = \frac{1}{N} \boldsymbol{\varepsilon}^{\mathrm{T}} \boldsymbol{\varepsilon}. \tag{28}$$

On average

$$E(\hat{\sigma}^2) = \sigma^2 \tag{29}$$

where $E(\cdot)$ is the expected value operator [17, p. 55]. Using $\hat{\varepsilon}_i$ to approximate ε_i and making use of equation (24) we obtain

$$E(\text{SSE}) \simeq N\sigma^2 \tag{30}$$

where N is the number of measurements. That is (average of SSE)/N is approximately equal to the variance, σ^2. If N is large enough, a particular value of the random variable SSE/N is usually close to its approximate mean value σ^2. Therefore, a criterion for selecting the basis for $\hat{f}$ is

$$\sqrt{(\text{SSE}/N)} \simeq \sigma. \tag{31}$$

A similar analysis applies in the case of correlated errors. For example, consider steady-state first-order autoregressive errors described by the model [18]

$$\varepsilon_i = \rho\varepsilon_{i-1} + u_i; \quad \varepsilon_0 \equiv 0 \tag{32a}$$

$$E(u_i) = 0 \tag{32b}$$

$$E(u_i u_j) = \begin{cases} 0, & i \neq j \\ \dfrac{\sigma_u^2}{1-\rho^2}, & i = j = 1 \\ \sigma_u^2, & i = j \neq 1 \end{cases} \tag{32c}$$

where u_i is a random variable and ρ and σ_u are considered known. In this case, criterion (31) is still applicable provided σ^2 is evaluated from

$$\sigma^2 = \frac{\sigma_u^2}{1-\rho^2}; \quad \rho^2 < 1. \tag{33}$$

In either case, an iterative process is needed in order to determine the surface temperature, $\hat{f}(t)$, and the surface heat flux, $\hat{q}(t)$. The procedure is as follows.

(1) Choose the spline parameters $\hat{k}$, $\hat{v}$, $\hat{\xi}_i$ and $\hat{I}$.
(2) Determine the appropriate spline functions, $\hat{B}^*$, and the interior basis functions, $\hat{D}^*$.
(3) Compute the coefficients $\hat{c}^*$ from equation (26).
(4) Compute SSE from equation (24).
(5) Compare $\sqrt{(\text{SSE}/N)}$ with the known value of the standard deviation, σ, of the measurements (given or computed from equation (33)). Repeat the above computations with a different choice of the spline parameters until sufficient agreement is obtained between $\sqrt{(\text{SSE}/N)}$ and σ as required by equation (31).
(6) Compute the estimated surface temperature, $\hat{f}(t)$, from equation (27).
(7) Compute the estimated surface heat flux, $\hat{q}(t)$, from equation (21).

In the present analysis, we choose to fix $\hat{k}$ and $\hat{v}_i$ and require evenly spaced intervals, but alter $\hat{I}$ in the above algorithm to satisfy equation (31). Note that the estimation of $\hat{f}$ is nonlinear due to equation (31).

4. ERROR ANALYSIS

The characteristics of the estimated surface temperature are now investigated. In the following approximate analysis, $\hat{n}^*$ and the functions $\hat{B}_j^*(t)$ are considered fixed so the effect of criteria (31) on the estimated temperature is being neglected. The measurement errors are assumed to have zero means, but, no assumptions are made concerning correlation or the distribution of the errors yet. The mean value of $\hat{f}$ is obtained by taking the expected value of equation (27) and noting that $E(\tilde{\mathbf{T}}) = \mathbf{T} = \mathbf{D}^{*\mathrm{T}}\mathbf{c}^*$.

$$E(\hat{f}) = \hat{\mathbf{B}}^{*\mathrm{T}}(\hat{\mathbf{D}}^*\hat{\mathbf{D}}^{*\mathrm{T}})^{-1}(\hat{\mathbf{D}}^*\mathbf{D}^{*\mathrm{T}})\mathbf{c}^* \tag{34}$$

and the variance becomes

$$\sigma_{\hat{f}}^2 \equiv E[(\hat{f} - E(\hat{f}))^2] = \hat{\mathbf{B}}^{*\mathrm{T}}(\hat{\mathbf{D}}^*\hat{\mathbf{D}}^{*\mathrm{T}})^{-1}\hat{\mathbf{D}}^* E(\boldsymbol{\varepsilon}\boldsymbol{\varepsilon}^{\mathrm{T}})\hat{\mathbf{D}}^{*\mathrm{T}}(\hat{\mathbf{D}}^*\hat{\mathbf{D}}^{*\mathrm{T}})^{-1}\hat{\mathbf{B}}^* \tag{35}$$

where $E(\cdot)$ is the expected value operator. Similar expression can be obtained for the estimated heat flux, $\hat{q}(t)$, by replacing $\hat{B}_j^*(t)$ with $-\partial\hat{d}_j^*(1,t)/\partial t$ in equations (34) and (35). For the additional standard assumptions of independent, constant variance errors

$$E(\boldsymbol{\varepsilon}\boldsymbol{\varepsilon}^{\mathrm{T}}) = \sigma^2\mathbf{I} \tag{36a}$$

where $\mathbf{I}$ is the identity matrix and equation (35) simplifies to

$$\sigma_{\hat{f}}^2 = \sigma^2\hat{\mathbf{B}}^{*\mathrm{T}}(\hat{\mathbf{D}}^*\hat{\mathbf{D}}^{*\mathrm{T}})^{-1}\hat{\mathbf{B}}^*. \tag{36b}$$

For the case of correlated errors given by equations (32)

$$E(\boldsymbol{\varepsilon}\boldsymbol{\varepsilon}^{\mathrm{T}}) = \sigma^2\mathbf{G} \tag{37a}$$

where the matrix $\mathbf{G}$ is defined by

$$\mathbf{G} = \begin{bmatrix} 1 & \rho & \rho^2 & \cdots \\ \rho & 1 & \rho & \cdots \\ \rho^2 & \rho & 1 & \cdots \\ \vdots & \vdots & \vdots & \end{bmatrix} \tag{37b}$$

and the variance becomes

$$\sigma_{\hat{f}}^2 = \sigma^2\hat{\mathbf{B}}^{*\mathrm{T}}(\hat{\mathbf{D}}^*\hat{\mathbf{D}}^{*\mathrm{T}})^{-1}\hat{\mathbf{D}}^*\mathbf{G}\,\hat{\mathbf{D}}^{*\mathrm{T}}(\hat{\mathbf{D}}^*\hat{\mathbf{D}}^{*\mathrm{T}})^{-1}\hat{\mathbf{B}}^*. \tag{37c}$$

Now we compare the estimated surface temperature, $\hat{f}$, with the exact surface temperature, f. The total error between the estimated and exact surface temperatures is composed of two parts

$$\hat{f} - f = [\hat{\mathbf{B}}^{*\mathrm{T}}(\hat{\mathbf{D}}^*\hat{\mathbf{D}}^{*\mathrm{T}})^{-1}(\hat{\mathbf{D}}^*\mathbf{D}^{*\mathrm{T}}) - \mathbf{B}^{*\mathrm{T}}]\mathbf{c}^* + \hat{\mathbf{B}}^{*\mathrm{T}}(\hat{\mathbf{D}}^*\hat{\mathbf{D}}^{*\mathrm{T}})^{-1}\hat{\mathbf{D}}^*\boldsymbol{\varepsilon}. \tag{38}$$

The first and second parts of this expression on the right-hand side are characterized as the deterministic stochastic errors, respectively

$$\text{det}(\hat{f}) \equiv [\hat{\mathbf{B}}^{*\mathrm{T}}(\hat{\mathbf{D}}^*\hat{\mathbf{D}}^{*\mathrm{T}})^{-1}(\hat{\mathbf{D}}^*\mathbf{D}^{*\mathrm{T}}) - \mathbf{B}^{*\mathrm{T}}]\mathbf{c}^* \tag{39}$$

$$\text{sto}(\hat{f}) \equiv \hat{\mathbf{B}}^{*\mathrm{T}}(\hat{\mathbf{D}}^*\hat{\mathbf{D}}^{*\mathrm{T}})^{-1}\hat{\mathbf{D}}^*\boldsymbol{\varepsilon}. \tag{40}$$

Therefore, equation (38) can be recast as

$$\hat{f} = f + \det(\hat{f}) + \text{sto}(\hat{f}). \tag{41}$$

These relations imply that the total error is composed of two parts: the deterministic and the stochastic error. When $\varepsilon = 0$ the stochastic error is zero and the total error is purely deterministic error. Also, the average total error, $E(\hat{f} - f)$, becomes

$$E(\hat{f} - f) = \det(\hat{f}) \tag{42}$$

since $E[\text{sto}(\hat{f})]$ vanishes. Therefore, $\det(\hat{f}(t))$ has two interpretations

$$\det(\hat{f}) = \begin{pmatrix}\text{total error when exact measurements}\\ \text{are input to the inverse analysis}\end{pmatrix} \tag{43a}$$

and

$$\det(\hat{f}) = \begin{pmatrix}\text{average total error when inexact}\\ \text{measurements are input to the}\\ \text{inverse analysis}\end{pmatrix}. \tag{43b}$$

When $f(t)$ and $\hat{f}(t)$ have the same functional form, the deterministic error is zero and the total error is purely stochastic error. The variance of $\text{sto}(\hat{f}(t))$ is the same as the variance of $\hat{f}(t)$. The above analysis can just as easily be applied to the estimated surface heat flux, $\hat{q}(t)$.

Now consider the development of confidence bounds on the estimated surface quantities. First, consider the standard assumptions of independent, constant variance, normally distributed, zero mean errors. We note from equation (27) that the estimated surface temperature is a normally distributed variable since it is a linear combination of the independent normal measurements. Since the distribution of $\hat{f}(t)$ is known to be normal, 99% confidence bounds are readily obtained for $\hat{f}(t)$ as

$$\text{Probability of } \{\hat{f} - \det(\hat{f}) - 2.576\sigma_{\hat{f}} < f < \hat{f} - \det(\hat{f}) + 2.576\sigma_{\hat{f}}\} = 99\% \tag{44}$$

where $\sigma_{\hat{f}}$ is given by equation (36b). When the deterministic error, $\det(\hat{f}(t))$, is neglected, equation (44) reduces to

$$\text{Probability of } \{\hat{f} - 2.576\sigma_{\hat{f}} < f < \hat{f} + 2.576\sigma_{\hat{f}}\} \simeq 99\%. \tag{45}$$

This relationship is used to determine the confidence bounds for the surface temperature, i.e. namely, $\hat{f}$ is computed from equation (27), $\sigma_{\hat{f}}$ from equation (36b) and 2.576 corresponds to 99% confidence bounds. Now consider steady-state, first-order, autoregressive correlated errors as described by equations (32) where u_i is normally distributed. In this case $\hat{f}$ is still normally distributed but with variance given by equation (37c). The corresponding confidence bounds are also given by equation (45) with $\sigma_{\hat{f}}$ now evaluated from equation (37c). Confidence bounds on $\hat{q}(t)$, for independent or correlated errors, are developed in the same manner.

The assumption of normally distributed errors in the preceding two cases is used to determine that $\hat{f}$ is also normally distributed. Once the distribution of $\hat{f}$ is known to be normal, the confidence bounds can be established. However, even if the errors are not exactly normal, $\hat{f}$ will be nearly normal anyway as a consequence of the central limit theorem of statistics [17, p. 167]. Basically, the theorem states that the distribution of $\hat{f}$ will be more normal than that of ε and in the limit, as the number of measurements tends to infinity, $\hat{f}$ becomes exactly normal (of course, if ε is normal then $\hat{f}$ is exactly normal for any number of measurements) [19]. Fortunately, normality in $\hat{f}$ is achieved very quickly; $\hat{f}$ is significantly non-normal only if the errors are extremely non-normal and only a few measurements are taken [20, pp. 21–23]. That is, relation (45) is not strongly dependent on the assumption of normal errors at all. We note that frequently extremely non-normal errors can be transformed to an approximately normal distribution with constant variance and then the preceding analysis is again applicable [20, p. 29]. In the event of extremely non-normal errors which cannot be transformed to near normality, distribution-free confidence bounds may be developed [20, p. 73].

5. RESULTS AND DISCUSSION

To illustrate the application of the present method of analysis on the use of periodic B-splines for the solution of quasi-steady periodic linear IHCP, we consider a plate of thickness unity subjected to zero temperature at the surface $x = 0$ and to a periodic temperature variation in the form of a square-wave at the surface $x = 1$. Suppose no prior information is available concerning the shape of $f(t)$. In this case, one might as well use uniform cubic periodic B-splines with full continuity conditions at the breakpoints as the basis for $\hat{f}(t)$; that is, choose

$$\hat{k} = 4 \tag{46a}$$

$$\hat{I} = \text{a variable parameter} \tag{46b}$$

$$\hat{\xi}_i = \text{evenly spaced intervals} \tag{46c}$$

$$\hat{v}_i = 3 \text{ continuity requirements.} \tag{46d}$$

We first examine the deterministic error involved in the estimation of the unknown surface temperature by the inverse analysis. In order to study the effect of the parameter $\hat{I}$ on accuracy, 30 evenly spaced exact temperatures at the centerline are chosen as the input data to the inverse analysis. Figure 1 shows the actual applied surface temperature in the form of a square-wave and the exact temperature measurements taken under quasi-steady conditions at the centerline $x = x_1 = 0.5$ of the slab. Figure 2 shows the estimated surface temperatures, computed using $\hat{n}^* = \hat{I} = 5$, 15 and 25 spline intervals, compared to the exact surface temperature. In view of equation (43a), the error in the estimated results is purely deterministic. Clearly

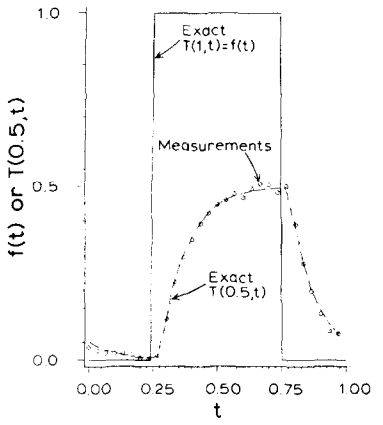

FIG. 1. Applied square-wave periodic surface temperature; exact interior temperature at $x = 0.5$; and 30 inexact simulated measurements at $x = 0.5$ with $\sigma = 0.01$.

as the number of spline intervals is increased, the quality of the estimation improves.

Next we consider the effects of random measurement errors on the estimated surface temperature. Due to lack of space we consider only the standard case of zero mean, constant variance, independent, normally distributed errors. The expected size of the stochastic error, sto $(\hat{f})$, is indicated by the normalized standard deviation, $\sigma_{\hat{f}}/\sigma = \sigma_{\text{sto}}(\hat{f})/\sigma$. Figure 3 illustrates the effect of measurement errors on the estimated surface temperature for $\hat{I} = 5$, 15 and 25. As the dimension (i.e. $\hat{n}^* = \hat{I}$) of the basis for $\hat{f}$ is increased, the estimated interior temperature more closely follows the measured data which contains error. Therefore, the sensitivity to measurement errors increases, as expected.

Now consider inexact input to the inverse analysis. Thirty simulated inexact measurements at $x_1 = 0.5$ with $\sigma = 0.01$ are used for the analysis as shown in Fig. 1. Since with increasing $\hat{I}$, the deterministic error decreases (Fig. 2) while the average stochastic error

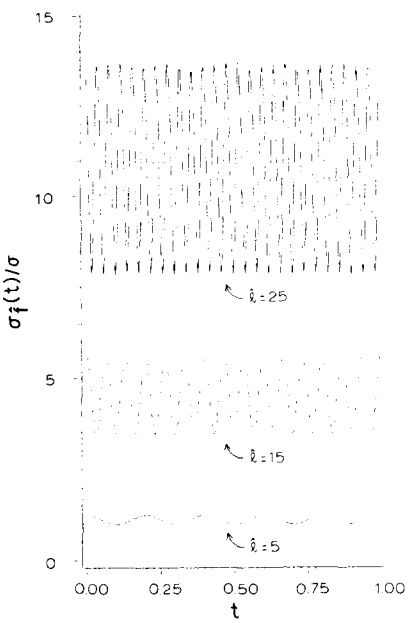

FIG. 3. Illustration of average stochastic error for cubic periodic B-splines with $\hat{I} = 5$, 15 and 25 intervals and full continuity conditions.

increases (Fig. 3), an optimal value of $\hat{I}$, which will minimize the total error, is expected to lie between the extreme values of 5 and 25 intervals. According to criteria (31) this optimal number, $\hat{I}_{\text{opt}}$, is approximately 16 and the corresponding estimated surface temperature is shown in Fig. 4(a). The r.m.s. estimated error, $\sqrt{(\text{SSE}/N)}$, calculated by taking $\hat{I} = 16$ is 0.0096 which differs from $\sigma = 0.0100$ by 4%. Also shown in Fig. 4(a) are the 99% confidence bounds on $\hat{f}$, based on equation (45). The approximate confidence bounds agree with the exact surface temperature except where the deterministic error is large as expected from equation (45).

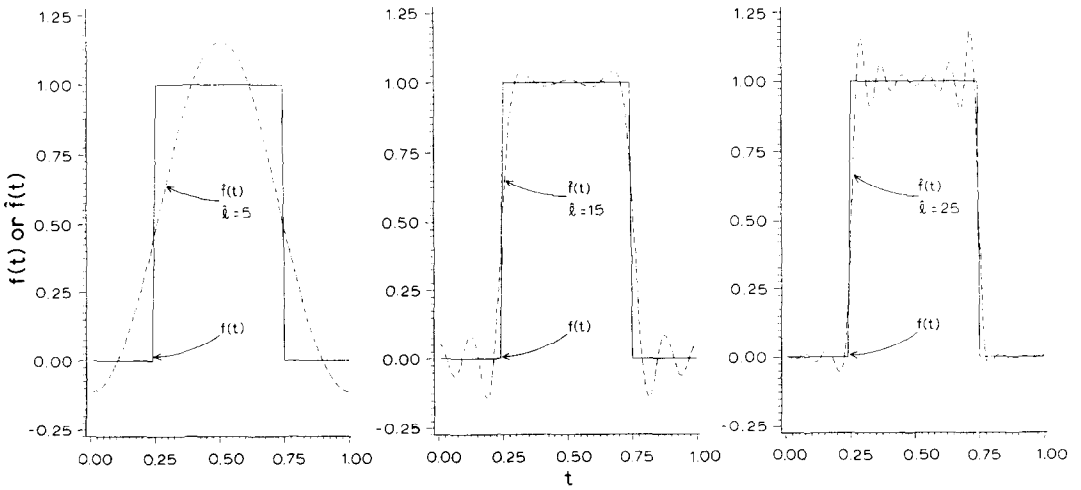

FIG. 2. Illustration of deterministic error for an applied square-wave surface temperature using cubic periodic B-splines with $\hat{I} = 5$, 15 and 25 intervals and full continuity conditions.

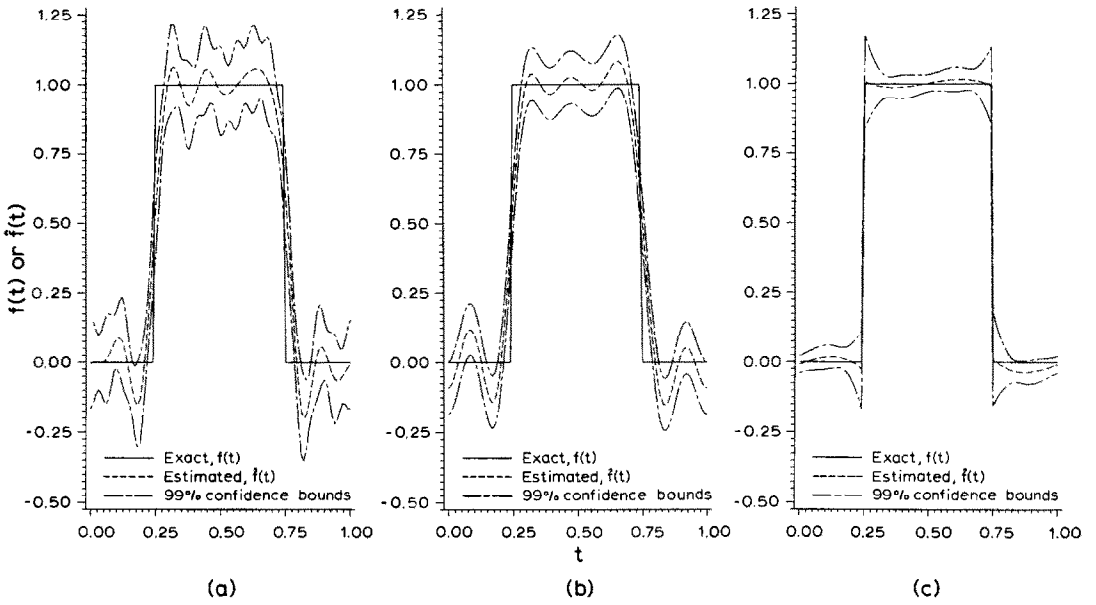

FIG. 4. Optimal estimated surface temperatures for an applied square-wave surface temperature and inexact measured data using: (a) cubic periodic B-splines with full continuity requirements, (b) a Fourier series representation and (c) cubic periodic B-splines with discontinuities specified at $t = 0.25$ and 0.75.

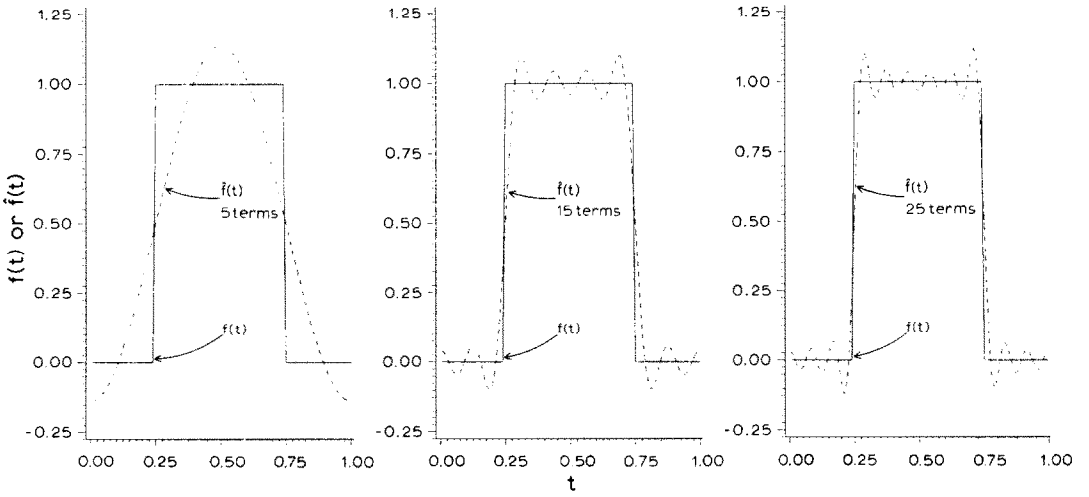

FIG. 5. Illustration of deterministic error for an applied square-wave surface temperature using a Fourier series representation using 5, 15 and 25 terms.

We now compare the present method using a periodic B-spline basis for $\hat{f}$ to the use a Fourier series basis in the form

$$\hat{f}(t) = \sum_{j=0}^{m} a_j \cos\left(\frac{2j\pi t}{\tau}\right) + \sum_{j=1}^{m} b_j \sin\left(\frac{2j\pi t}{\tau}\right). \quad (47)$$

Since a smooth B-spline representation has been specified (continuity through the second derivative), we expect the slightly more smooth Fourier series to produce results similar to the B-spline results. Figures 5 and 6 show the results analogous to those contained in Figs. 2 and 3, respectively, for the trigonometric basis as given by equation (47) for $(2m + 1) = 5$, 15 and 25 terms. Inspection of Figs. 2 and 5 indicates the periodic B-spline approach is at least as good as the Fourier series method in minimizing the deterministic error. Note that the oscillations near the discontinuities die out more quickly when periodic B-splines are used since continuity in the higher order derivatives is not required. Comparison of Figs. 3 and 6 shows that the average size of the stochastic error is the same for both approaches. When data with measurement error is used, the optimal estimated surface temperatures, as selected by criteria (31), agree also as shown by Figs. 4(a) and (b). Therefore, when prior information about $f(t)$ is not available and a smooth, uniform periodic B-spline basis is specified,

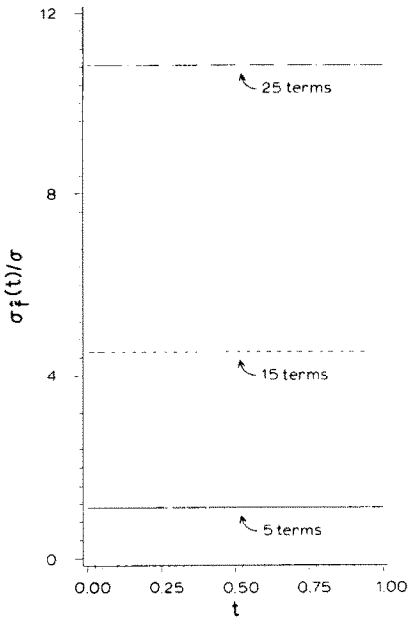

FIG. 6. Illustration of average stochastic error for a Fourier series representation using, 5, 15 and 25 terms.

the present approach can effectively reproduce the Fourier series results.

Consider now a situation in which the true surface temperature is known to have discontinuities. Suppose that the surface temperature of Fig. 1 is the result of a periodic on–off heating process for which the duration of each process is known. In this case, we incorporate this prior information into the B-spline basis by requiring breakpoints at $t = 0.25$ and 0.75 with $v = 0$ continuity conditions. Figure 4(c) shows the results when inexact data is input to the inverse analysis with the selections $\hat{k} = 4$, $\hat{I} = 3$, $\hat{\xi}_i = \{0, 0.25, 0.75, 1.00\}$ and $\hat{v}_i = \{4, 0, 0, 4\}$ chosen to best satisfy criteria (31). Clearly, applications with a known discontinuous surface temperature are better treated with a periodic B-spline basis than a Fourier series approach, as shown by Figs. 4(b) and (c). (Actually, criteria (31) indicated that even the current model with $\hat{k} = 4$ and using only $\hat{I} = 3$ is too flexible since it leads to a value of $\sqrt{(\text{SSE}/N)}$ of about 0.0068, which is significantly less than $\sigma = 0.0100$, for these selections of the parameters. In this case, the order of the spline functions, $(\hat{k} - 1)$, should be reduced to further optimize the estimation of $f(t)$.)

Finally, we consider an example in which prior information about the general shape of the unknown surface temperature, $f(t)$, can be used with a periodic B-spline basis to achieve improved results over the sine–cosine representation through a reduction in the number of parameters in the model for $\hat{f}(t)$. In Fig. 7(a) an arbitrary simulated periodic wall temperature variation with an abrupt change is illustrated. Suppose 20 measurements with error level $\sigma = 0.1$ are taken at $x_1 = 0.05$ as shown in Fig. 7(a). We base our selection of the B-spline representation of $\hat{f}(t)$ on the following prior knowledge about $f(t)$.

(1) A sharp temperature spike occurs between approximately $t = 0.45$ and 0.55.

(2) Otherwise the temperature variation is smooth.

The above information motivates the following B-spline basis

$$\hat{k} = 4 \tag{48a}$$

$$\hat{I} = 5 \tag{48b}$$

$$\hat{\xi}_i = \{0, 0.20, 0.45, 0.55, 0.75, 1.00\} \tag{48c}$$

$$\hat{v}_i = \{3, 3, 2, 2, 3\}. \tag{48d}$$

Since sharp curvature is expected near $t = 0.45$ and at 0.55, continuity of the second derivatives is not required in relations (48). The B-spline results are shown in Fig. 7(b) while the Fourier series results are given in Fig. 7(c). The dimension of the B-spline basis given by equations (48) is $N_d = \hat{n}^* = 7$ while the number of terms required by basis given by equation (47) to achieve the same degree of fit in terms of the SSE is 13. Since the Fourier representation is very smooth, more terms were required to fit the near discontinuity at $t = 0.5$ than the less smooth B-spline basis. The increased sensitivity of the Fourier series approach is evident from the broader confidence bounds in Fig. 7(c). Clearly the B-spline results are better than the Fourier series results since prior information about $f(t)$ has been incorporated into the B-spline representation of $\hat{f}(t)$ to reduce the number of parameters.

6. CONCLUSIONS

The periodic B-spline/integral transform approach has been developed to solve linear inverse heat conduction problems involving a periodically varying unknown surface temperature at one of the boundary surfaces. Problems involving discontinuities or abrupt variations in the surface temperature can readily be handled with the present method. When some information is available regarding the general functional form of the applied surface temperature, such information can be incorporated in the B-spline basis to reduce sensitivity to measurement errors. The method is also capable of handling smooth variations in the applied surface temperature as effectively as the Fourier series approach.

Acknowledgements—This material is based upon work supported under a National Science Foundation Graduate Fellowship. This work was supported in part through the National Science Foundation Grant MEA 83-13301.

REFERENCES

1. A. C. Alkidas, Heat transfer characteristics of a spark-ignition engine, *J. Heat Transfer* **102**, 189–193 (1980).
2. V. D. Overbye, J. E. Bennethum, O. A. Uyehara and P. S. Myers, Unsteady heat transfer in engines, *SAE Trans.* **69**, 461–494 (1961).

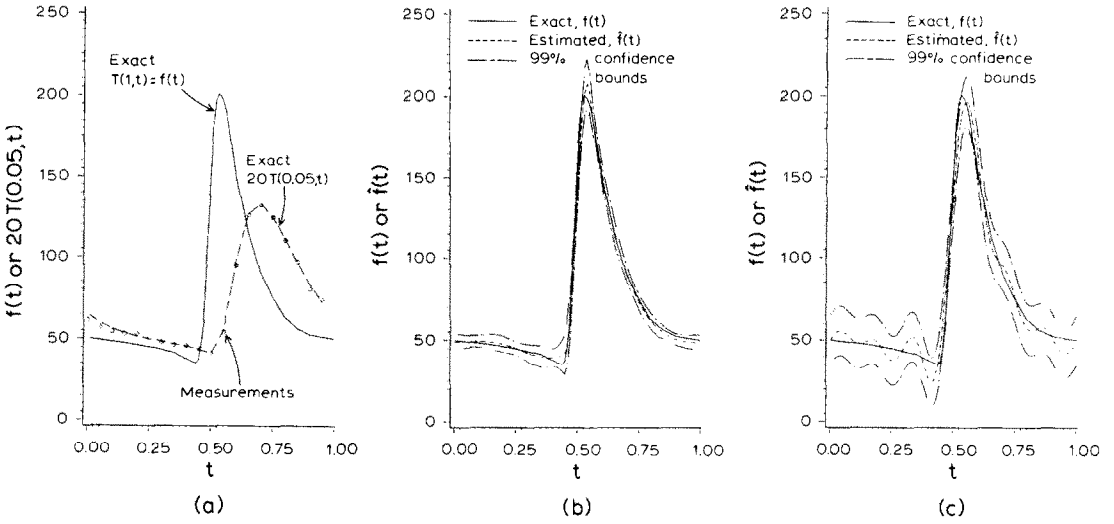

FIG. 7. (a) Simulated abrupt wall temperature variation and 20 inexact measurements at $x = 0.05$ with $\sigma = 0.1$ along with the corresponding optimal estimated surface temperatures using a (b) B-spline basis and (c) Fourier series basis.

3. D. J. McKinzie, Jr., Experimental confirmation of cyclic thermal joint conductance, AIAA-paper 70-853 (1970).
4. J. R. Howard, An experimental study of heat transfer through periodically contacting surfaces, *Int. J. Heat Mass Transfer* **19**, 367–372 (1976).
5. J. C. Hein, Heat conduction in a plane wall subject to periodic temperature changes, *Warme- und Stoffubertragung* **18**, 61–67 (1984).
6. S. J. Putterman and R. Guibert, Enhancement of diffusive transfer by periodic pulsation between Dirichlet and Neumann type boundary conditions, *Appl. Scient. Res.* **40**, 271–277 (1983).
7. D. W. Wendland, The effect of periodic pressure and temperature fluctuations on unsteady heat transfer in a closed system, NASA-Report CR-72323 (1968).
8. D. M. France and T. Chiang, Analytic solution to inverse heat conduction problems with periodicity, *J. Heat Transfer* **102**, 579–581 (1980).
9. W. A. Updike, Computation of surface temperatures for time dependent periodic convection boundary conditions, ASME-paper 84-WA/HT-40 (1984).
10. M. D. Mikhailov, Quasi-steady state temperature distribution in finite regions with periodically varying boundary conditions, *Int. J. Heat Mass Transfer* **17**, 1475–1478 (1974).
11. J. V. Beck, Calculation of surface heat flux from an internal temperature history, ASME-paper 62-HT-46 (1962).
12. E. Hensel and R. G. Hills, An initial value approach to the inverse heat conduction problem, *J. Heat Transfer* **108**, 248–256 (1986).
13. M. Raynaud and J. Bransier, A new finite-difference method for the nonlinear inverse heat conduction problem, *Numer. Heat Transfer* **9**, 27–42 (1986).
14. M. N. Ozisik, *Heat Conduction*, pp. 311–314. Wiley, New York (1980).
15. C. de Boor, *A Practical Guide to Splines*, Springer, New York (1978).
16. J. V. Beck, B. Blackwell and C. R. St. Clair, Jr., *Inverse Heat Conduction*, pp. 140–141. Wiley, New York (1985).
17. R. E. Walpole and R. H. Myers, *Probability and Statistics for Engineers and Scientists* (2nd edn). McMillan, New York (1978).
18. J. V. Beck and K. J. Arnold, *Parameter Estimation in Engineering and Science*, pp. 303–306. Wiley, New York (1977).
19. R. Caulcutt, *Statistics in Research and Development*, p. 269. Chapman & Hall, London (1983).
20. O. L. Davies and P. L. Goldsmith (editors), *Statistical Methods in Research and Production* (4th edn). Oliver & Boyd, Edinburgh (1972).

APPENDIX

The following type of integral appears twice in equation (15b)

$$\int_{t_1}^{t_2} \exp[r(t-v)]B_{i,k}(t)\,dt \tag{A1}$$

where $(k-1)$ is the order of the spline functions. Let **s** denote the knot sequence defining the B-splines [15, pp. 119, 321]. Since $B_{i,k}(t)$ is a different polynomial on each interval (s_{i+j-1}, s_{i+j}), $j = 1, 2, \ldots, k$, split up integral (A1) as

$$\sum_{j=1}^{k} \int_{\max(t_1, s_{i+j-1})}^{\min(t_2, s_{i+j}-\delta)} \exp[r(t-v)]\,B_{i,k}(t)\,dt \tag{A2}$$

where δ is a small number. Define

$$z_{2j} \equiv \min(t_2, s_{i+j} - \delta) \tag{A3a}$$

$$z_{1j} \equiv \max(t_1, s_{i+j-1}) \tag{A3b}$$

and consider each integral

$$\int_{z_{1j}}^{z_{2j}} \exp[r(t-v)]\,B_{i,k}(t)\,dt \tag{A4}$$

appearing in integral (A2) separately. Since $B_{i,k}(t)$ is a continuous function for $z_{1j} \le t \le z_{2j}$, integral (A4) can be integrated by parts as

$$\frac{1}{r}\exp[r(t-v)]\,B_{i,k}(t)\Big|_{z_{1j}}^{z_{2j}} - \int_{z_{1j}}^{z_{2j}} \frac{1}{r}\exp[r(t-v)]\frac{d}{dt}B_{i,k}(t)\,dt. \tag{A5}$$

The derivative of the B-spline is evaluated from the recursion formula [15, p.139]

$$\frac{\mathrm{d}}{\mathrm{d}t}B_{i,k}(t) = (k-1)\left[\frac{B_{i,k-1}(t)}{s_{i+k-1}-s_i} - \frac{B_{i+1,k-1}(t)}{s_{i+k}-s_{i+1}}\right]. \quad \text{(A6)}$$

Hence

$$\int_{z_{1j}}^{z_{2j}} \exp[r(t-v)]\,B_{i,k}(t)\,\mathrm{d}t = \frac{1}{r}\left\{\exp[r(t-v)]\,B_{i,k}(t)\Big|_{z_{1j}}^{z_{2j}} - \frac{k-1}{s_{i+k-1}-s_i}\int_{z_{1j}}^{z_{2j}} \exp[r(t-v)]\,B_{i,k-1}(t)\,\mathrm{d}t + \frac{k-1}{s_{i+k}-s_{i+1}}\int_{z_{1j}}^{z_{2j}} \exp[r(t-v)]\,B_{i+1,k-1}(t)\,\mathrm{d}t\right\}. \quad \text{(A7)}$$

The recursion formula (A7) is started from the values

$$\int_{z_{1j}}^{z_{2j}} \exp[r(t-v)]\,B_{i,1}(t)\,\mathrm{d}t = \frac{1}{r}\exp[r(t-v)]\Big|_{\max(z_{1j},s_i)}^{\min(z_{2j},s_{i+1}-\delta)}$$

$$\text{if } \min(z_{2j}, s_{i+1}-\delta) > \max(z_{1j}, s_i) \quad \text{(A8a)}$$

$$= 0 \quad \text{otherwise.} \quad \text{(A8b)}$$

Equations (A7) and (A8) provide a complete recursion relation for the evaluation of integral (A4). Expression (A2) is then used to compute integral (A1).

METHODE B-SPLINE PERIODIQUE POUR LE PROBLEME INVERSE DE LA CONDUCTION PERIODIQUE ETABLIE

Résumé—Une approche basée sur l'utilisation de la méthode B-spline et sur la transformée intégrale est proposée pour résoudre les problèmes linéaires inverses de la conduction thermique périodique établie. Les approches précédentes basées sur une représentation en série finie de Fourier de la condition inconnue sur la surface conviennent mieux aux variations lentes. Mais en utilisant une représentation B-spline, des problèmes avec des discontinuités ou des variations rapides de la condition à la surface peuvent être traités. La souplesse de la base B-spline fournit une information concernant le comportement fonctionnel général de la condition de surface pour être mieux introduite dans le modèle.

PERIODISCHES B-SPLINE-VERFAHREN ALS GRUNDLAGE ZUR BESCHREIBUNG QUASISTATIONÄRER, PERIODISCHER, INVERSER WÄRMELEITVORGÄNGE

Zusammenfassung—Es wird eine Methode zur Lösung quasistationärer, periodischer, linearer, inverser Wärmeleitvorgänge mit Hilfe periodischer B-Splines und der Integral-Transformationstechnik vorgeschlagen. Ein früher vorgestelltes Verfahren, bei dem die unbekannte Oberflächenbedingung mit Hilfe einer Fourier-Reihe dargestellt wurde, eignet sich sehr gut, um zeitliche Änderungen der Oberflächenbedingung anzupassen. Durch Verwenden der B-Spline-Methode können jetzt auch Unstetigkeiten oder plötzliche Änderungen der Oberflächenbedingung ohne Schwierigkeiten behandelt werden. Die Beweglichkeit des B-Spline-Verfahrens erlaubt es, mehr Vorabinformation (bezüglich des allgemeinen Verhaltens der Oberflächenbedingung) besser in das Modell zu integrieren.

ПЕРИОДИЧЕСКИЙ В-СПЛАЙН ДЛЯ РЕШЕНИЯ КВАЗИСТАЦИОНАРНЫХ ПЕРИОДИЧЕСКИХ ОБРАТНЫХ ЗАДАЧ ТЕПЛОПРОВОДНОСТИ

Аннотация—Метод, основанный на использовании периодических В-сплайнов и методике интегрального преобразования, предлагается для решения квазистационарных периодических линейных обратных задач теплопроводности. Ранее применявшиеся подходы базируются на представлении неизвестных условий на поверхности в виде конечного ряда Фурье, хорошо соответствуют монотонному изменению во времени условий на поверхности. Использование В-сплайнов дает возможность эффективно решать задачи с разрывными и резко изменяющимися условиями на поверхности. Универсальность В-сплайнов позволяет более адекватно модели использовать информацию об условиях на поверхности.